Shaped Pupil Coronagraph: State of the Art and Projections for TPF Performance and Readiness

N. J. Kasdin (PI)[1], R. Belikov[1], E. Cady[1], M. Carr[1], J. Kay[1], M. Littman[1], L. Pueyo[1], R. J. Vanderbei[1], J. T. Trauger (PI)[2], K. Balasubramanian[2], P. Echternach[2], A. Give'on[2], A. Kuhnert[2], S. Shaklan[2], F. Shi[2], A. R. Neureuther (PI)[3], D. Ceperley[3], M. Miller[3], T. Shih[3], S. Kilston[4], M. Lieber[4], and J. Beall[5]

[1]Princeton University, [2]Jet Propulsion Laboratory, California Instiute of Technology, [3]Univeristy of California, Berkeley, [4]Ball Aerospace, and [5]NIST

ABSTRACT

The Shaped Pupil Coronagraph (SPC) is a high-contrast imaging system pioneered at Princeton and designed for the TPF-C telescope. In this document, we summarize the work done to date on the SPC to date and evaluate its current and projected performance. What makes the SPC attractive for TPF is that it is very simple to make and set up, and it is inherently broadband. Owing to the simplicity of the SPC, it is quickly becoming a relatively mature technology with theoretical and experimental validations of its performance. Many shaped pupils have been designed to various specifications and tools are in place to quickly turn out more. Full vector-field simulations show that realistic shaped pupils can already achieve 10^{10} contrast in the absence of aberrations. A manufacturing process has been developed to make shaped pupils for as little as a few thousand dollars, at JPL and NIST. Shaped pupils have also been shown to be very insensitive to aberrations, and especially low order aberrations such as tilt and defocus. The SPC is undergoing extensive studies in the lab, and so far a suppression of 4×10^{-8} has been achieved in 10% broadband light (averaged across a region between 4 and 9 λ/D), after speckle-nulling-based wavefront correction. The limiting factor is now believed to be well-understood and is primarily the inability of the speckle nulling algorithm to correct for manufacturing errors in the mask. It was shown that this limitation can be overcome by using a more sophisticated estimation algorithm called peak-a-boo, or by using a shaped pupil design that is insensitive to manufacturing defects. The SPC lends itself well to many wavefront estimation and correction schemes. Simulations show that realistic shaped pupil manufacturing errors and realistic wavefront error can be corrected with a single DM at one wavelength, and 2 or 3 DMs in broadband. The main disadvantages of the SPC is throughput, sharpness, and working angle, but the throughput disadvantage may be counterbalanced to an extent by the fact that SPC requires very few optical components and the fact that the light blocked by the mask may still be used to sense aberrations.

INTRODUCTION

The Shaped Pupil Coronagraph (SPC) is a high-contrast imaging system under development at Princeton, designed for NASA's Terrestrial Planet Finder Coronagraph (TPF-C) mission[1]. The SPC is a type of an apodized-pupil coronagraph, where high contrast is achieved simply by apodizing the telescope pupil by a binary mask (the shaped pupil). Many shaped pupil designs can be found with high-contrast point spread functions (PSFs) that meet the TPF requirements of 10^{10} contrast at an inner working angle of 4 λ/D. Because the only required component in an SPC is a shaped pupil mask, the SPC is very simple and cheap to make, trivial to align, and is inherently broadband. Lab validations of the SPC are progressing and to date have shown it to be relatively close to the TPF requirements in broadband light. The main disadvantages of the SPC are its theoretically low throughput and limited discovery space. However, any considerations of throughput must also take into account practical issues such as number of required optical elements, bandwidth, and whether the "lost" photons can still be used. The SPC in principle only requires one optical element: the primary, it is inherently broadband, and the photons blocked by the shaped pupil can actually be utilized to help estimate aberrations.

Therefore, the SPC's low theoretical throughput may in fact be counterbalanced by gains in this practical throughput.

A rough schematic of the baseline option of the TPF-C telescope with an SPC and a wavefront correction system is shown in Figure 1. The system consists of the TPF telescope, followed by the wavefront correction system and the SPC. The wavefront correction system can be designed to a large extent independently of the SPC, so we do not show its details here. The SPC consists of the shaped pupil at a reimaged pupil plane, and the science camera with an optional star occulter if the camera itself is incapable of properly accepting light intensity with a 10^{10} dynamic range. The star occulter is a hard-edged mask designed to block the brightest portions of the PSF. If the star occulter cannot be placed very close to the chip, the science camera can be placed at a reimaged image plane downstream from the star occulter. Aside from imaging planets, the science camera will also be used to estimate aberrations and feed this estimation data back to the wavefront correction system (additional cameras can also be used for this purpose).

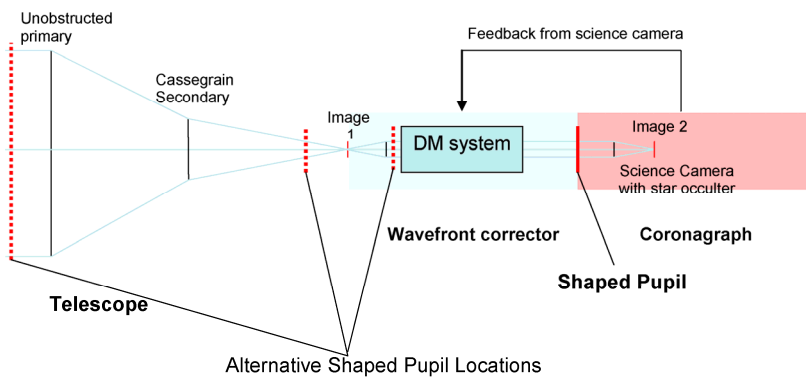

Figure 1: *Simplified schematic diagram of the TPF telescope with a shaped pupil coronagraph. The shaped pupil can be placed in virtually any "pupil" plane*

Even though our baseline position for the shaped pupil is as shown by the solid line in Figure 1, the shaped pupil can be located in many other planes, such as those indicated by the dotted lines. In fact, one attractive design is a single-mirror prime-focus telescope with a shaped pupil either in front of the primary or along the converging beam downstream. Such a prime-focus design is attractive not only because it is so simple, but also because it eliminates light losses and aberrations introduced by all optics except for the primary. (In fact, this design has no phase-induced amplitude or similar aberrations.) However, the prime-focus design may not be practical because it requires the ability to shape the primary to be free of aberrations and a few other technical challenges.

SHAPED PUPIL DESIGN AND MANUFACTURE

Shaped pupils are designed by specifying contrast as well as the areas in the PSF where this contrast is to be achieved (dark zones), and running nonlinear optimization techniques on the pupil shapes to optimize throughput[2]. Many pupil designs and design types were created over the years (see, e.g., Vanderbei et al. 2004[3]), but we have identified the so-called "ripple" design type as being the easiest to manufacture as a free-standing mask. Some of the designs we manufactured (by NIST and/or JPL[4]) are shown in Figure 2. The manufacturing process was deep reactive ion etching of silicon wafers. Mask were manufactured in both 10 and 25mm diameters. Ripple 1 was designed for the elliptical shape of TPF-C while ripple 3 was designed for a circular pupil. As could be seen by the horizontal cross-sections in the bottom row of Figure 2, both were designed to achieve better than 10^{-9} contrast at an inner working angle of $4\lambda/D$. Both have about 10% Airy throughput (i.e., the fraction of the input beam power that falls in the main lobe of the PSF). As could be seen from the PSFs in Figure 2, the dark zone for ripple 1 has 45° openings on two sides of the main lobe, and ripple 3 has 90° openings. As mentioned before, the theoretically low throughput of the shaped pupils can be compensated for to some extent by the fact that the SPC does not require any optics in addition to the shaped pupil, which eliminates losses due to reflections; and the fact that the SCP is inherently broadband, so that any photon losses due to narrow-band filtering are eliminated.

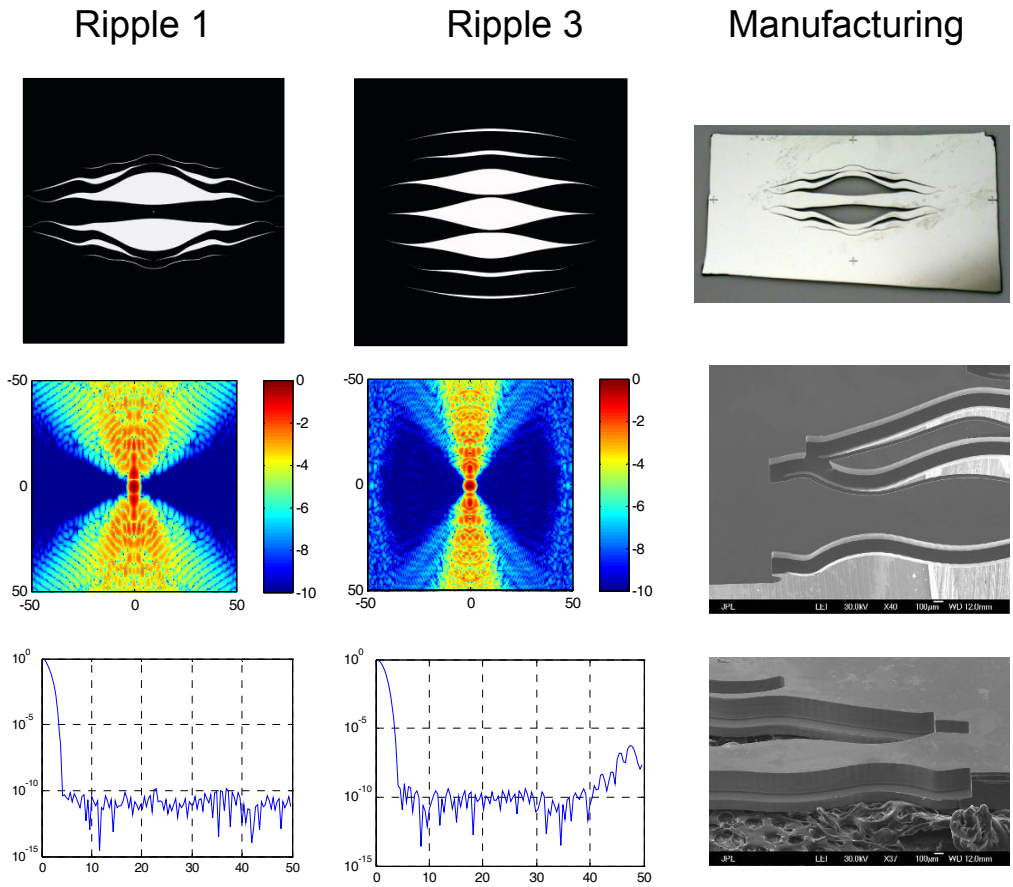

Figure 2: *Left two columns: examples of shaped pupil designs. Top row is the shaped pupil (white is transmissive); second row is the PSF, showing the high-contrast regions in blue; and third row is the horizontal slice through the PSF. All axes are in units of λ/D. Right column: microscope pictures of a manufactured mask.*

MASK SIMULATIONS

The shaped pupils are designed assuming that the masks will be ideal and that the image plane is an exact Fourier Transform of the pupil plane. One important question is whether these assumptions are valid in practice. In this section, we present the results of full vector simulations that show that in most cases of interest, these assumptions are indeed valid.

Ceperly et al.[5] have performed finite-difference-time-domain simulations of the interactions between the vector electro-magnetic fields and the edges of a realistic mask (i.e., real material, non-0 thickness) and compared the results to the assumption of an ideal mask (i.e., ideal apodization, 0 thickness). The main results are summarized in Figure 3. The left column specifies various cases that were simulated and the right column shows the magnitude of the difference between a real and an ideal mask (taking the worst case for the last 5 rows). By "vertical sidewalls", we mean the case where the edges of the mask have walls that form a 90 degree angle with respect to the substrate. By "20° undercut", we mean that this angle is 90°–20° (with the mask opening being narrower on the illuminated side of the mask). "Xμm opening" refers to the width of the mask opening in cross section. The value of the parameter on the right column (severity) corresponds to the width along the edge of the ideal mask that contains the same amount of energy as the perturbation due to the effect on the left column. The main conclusions of these simulations are that vertical sidewalls are to be avoided, and that small mask tilts, changes of polarization and wavelengths, and metal coatings are the least significant.

Mask Structure:	Severity:
Vertical sidewalls, Off-axis illumination, 10um Opening, 100um Thick	7 λ
Vertical sidewalls, Off-axis illumination, 10um Opening, 50um Thick	4 λ
Vertical sidewalls, On-axis illumination, 10um Opening, 100um Thick	3–4 λ
Vertical sidewalls, On-axis illumination, 10um Opening, 50um Thick	3 λ
Vertical sidewalls, On-axis illumination, 48um Opening, 50um Thick	3 λ
Vertical sidewalls, On-axis illumination, 48um Opening, 50um Thick	2–3 λ
20° undercut sidewalls, On-axis illumination, 48um Opening, 50um Thick	λ / 4
Physical effects on 50um thick Si masks with 48um openings at 630nm:	Worst case:
Undercut angle	3 λ
Small mask tilt	λ / 2 per degree tilt
Polarization	λ / 4
Wavelength (630nm to 785nm)	λ / 4
200nm Cr top-coat	λ / 100

Figure 3: *Extent of different effects on the fields around the edges.*

This data was used to study how vector interactions with the real mask affect the PSF of the real mask (Lieber et al[6]). The main conclusions were that severities of less than λ/4 do not degrade the 10^{10} contrast for mask sizes 10 cm and larger. Therefore, with a properly undercut mask, the mask can be assumed ideal and insensitive to polarization, wavelength changes, or coatings. For masks that are not undercut, the degradation depends on the mask type and size. In a 10 cm ripple mask, contrast is degraded to 10^9, while for a 10 cm checkerboard mask, contrast is not degraded. All such effects will be insignificant compared to wavefront error. One important corollary to this work is that manufacturing error or imprecision of the edges as large as λ/4 is insignificant (at least to the extent that manufacturing errors along the edges are similar to effective errors due to vector effects). Such an error is well within modern manufacturing tolerances. The results presented in this section indicate that real masks can be manufactured today which, in the absence of wavefront aberrations, will achieve the 10^{10} contrast required by TPF (except for the trimming limitation discussed later, which can be overcome by specialized mask designs).

SENSITIVITY TO WAVEFRONT ABERRATIONS

In order to assess the sensitivity of shaped pupils to wavefront aberrations, we simulated different Zernike aberrations at the pupil plane and studied their effects at the image plane[7,8]. Some of these results are summarized in Figure 4. For these simulations, we assumed a circular concentric ring shaped pupil. Each subplot corresponds to a different Zernike (starting from tilt, defocus, etc.), and shows the contrast in the image plane at a particular working angle (4 or 8 λ/D) as a function of RMS of aberration. Just as with many other coronagraphs, the sensitivity is more pronounced at lower inner working angles and higher Zernike orders. The main conclusion of this work, however, is that the SPC is very insensitive to aberrations (especially to pointing error or other forms of tilt, defocus, and astigmatism). The wavefront flatness requirement depends on the aberration, but assuming typical power spectral density fall-off such as $1/f^3$, the total flatness requirement needs to be on the order of λ/10,000.

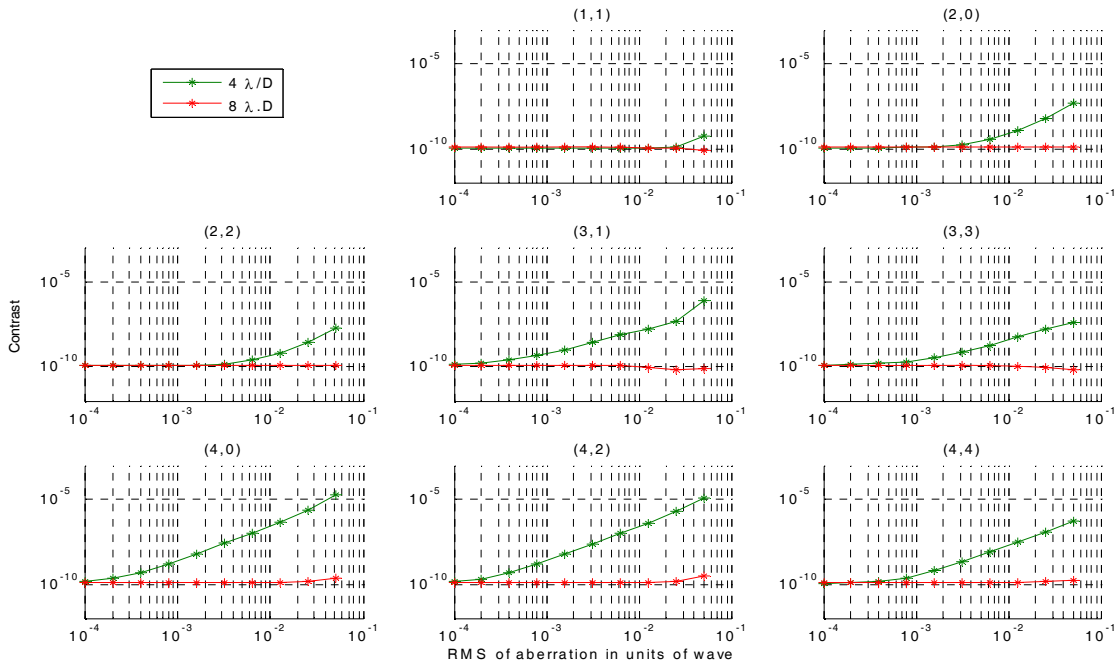

Figure 4: *Sensitivity to different Zernike aberrations for a concentric ring shaped pupil mask as a function of RMS of aberrations, at inner working angles of 4 and 8 λ/D. The title of each graph is the Zernike radial and azimuthal index.*

LABORATORY RESULTS

Experimental validation of shaped pupils is currently under way at Princeton and JPL[9,10]. The Princeton testbed is relatively new and low cost, consisting of an optical bench with an enclosure in a semi-clean room, and 2 recently acquired Boston Micromachines DMs. We are currently getting contrast levels of about 10^5 without wavefront correction and about 10^6 with wavefront correction. Both values hold for the largest bandwidth we tried, ~450–750 nm, demonstrating the broadband advantage of shaped pupils. Simulations indicate that the contrast-limiting factor for us is twofold. One, we are using a small mask (10 mm) because of the small size of our DM. Any manufacturing errors are proportionately greater for smaller masks, and in our case they appear at about 10^{-6} level. Two, the correction algorithm we are currently using, speckle nulling, is incapable of correcting for errors of this kind. Hence, we expect to be able to reach much better contrast if we either (a) adopt our setup to be able to accommodate a larger mask given the small DM without degrading contrast; (b) design a mask more tolerant to manufacturing limitations, or (c) use a more sophisticated correction algorithm such as peak-a-boo[11]. We are currently pursuing all three, with a focus on (c). Simulations show that peak-a-boo is capable of correcting for errors due to manufacturing defects which are beyond the ability of speckle nulling.

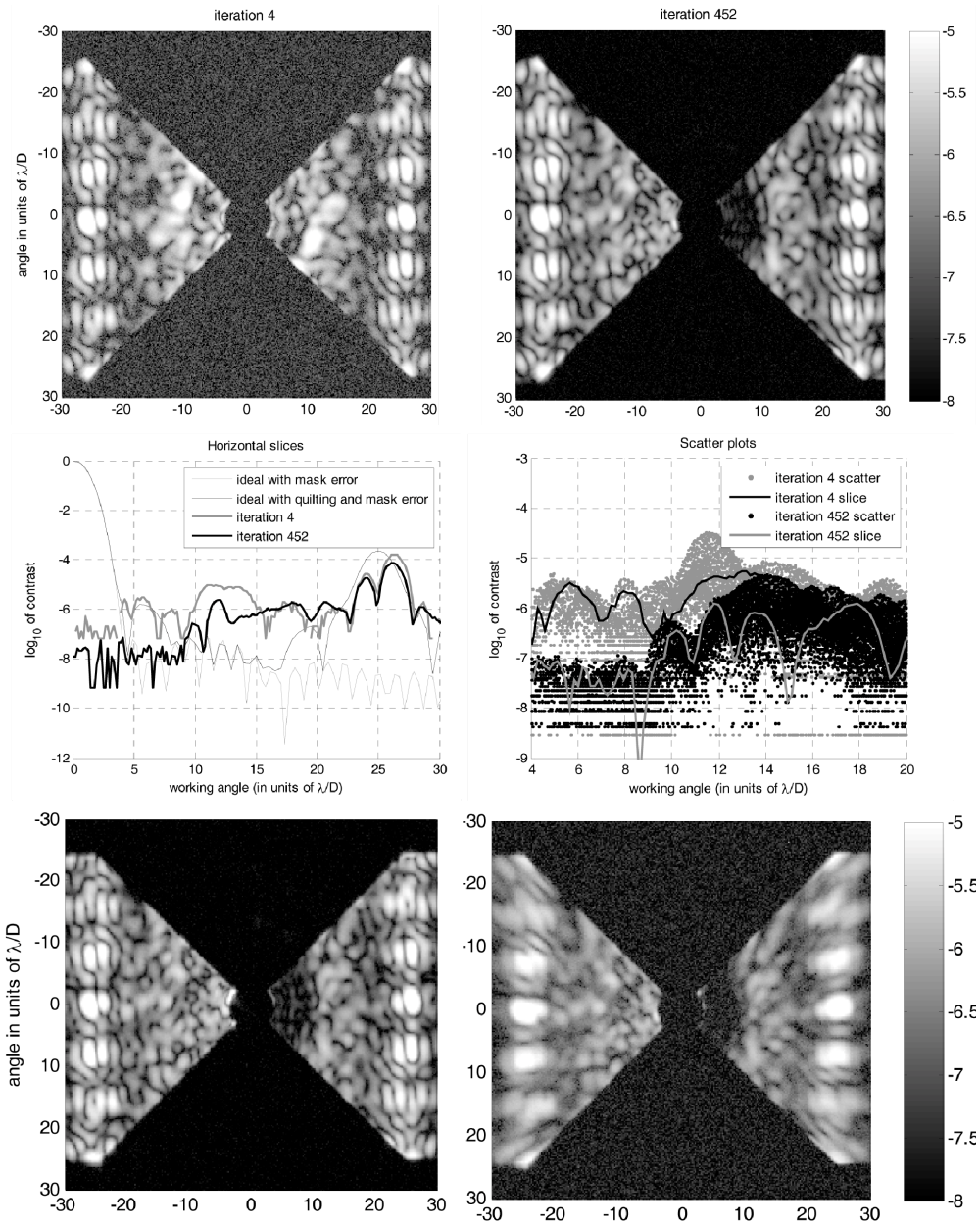

Figure 5: *Contrast plots from tests at the HCIT. Top left: one of the starting speckle nulling iterations (iteration 4) at 785 nm. Top right: one of the final iterations (iteration 452). The higher amount of noise in the image of iteration 4 is due to lower exposure time. Middle left: horizontal traces through the centers. Middle right: scatter plots in the dark region. Bottom left: after changing from 785- to 836-nm light. Bottom right: after changing to broadband light. For the λ/D scale, λ = 785 nm and D = 25 mm.*

JPL's testbed (HCIT), on the other hand, is somewhat more sophisticated than the one at Princeton, consisting of a vacuum chamber in a clean room and a having a large DM[12]. Owing to this, our best results to date are from an experiment performed at HCIT with a 25-mm shaped pupil, where we have achieved suppression of 4×10^{-8} with speckle nulling. Simulations show that this is about the level of contrast due to manufacturing limitations (trimming) for the particular shaped pupil we used. Work is progressing on a design and manufacturing process capable of yielding a mask with no significant manufacturing defects.

Our experimental setup at HCIT was designed to take an image of the PSF of the shaped pupil. A DM was present in a pupil plane upstream of the shaped pupil to correct for aberrations. A bowtie-shaped star occulter was used in an image plane upstream of the camera to prevent a lot of bright light hitting the CCD. Speckle nulling was performed at 785 nm and then the wavelength was switched to 836nm and to 760–840 nm broadband light. The results are shown in Figure 5. Without any corrections, the contrast on the HCIT testbed is similar to the Princeton testbed, or 10^5 at 4 λ/D (the HCIT system was already slightly corrected when we started, so that the starting point is closer to 10^6). After wavefront correction, the suppression is 4×10^{-8} between 4 and 9 λ/D (averaged across the dark region). As can be seen from Figure 5, this contrast is maintained after switching to either 836nm or broadband light, once again demonstrating achromaticity of shaped pupils.

WAVEFRONT SENSING AND CONTROL

Speckle nulling is a very robust and simple method of wavefront correction, but it has certain limitations, notably speed and inability to correct for certain kinds of aberrations. More sophisticated methods are necessary for use in space. Many correction methods are being developed for or can be adopted for use with the SPC. The hardware necessary for various methods is outlined in Figure 6, along with a few notes on each method. The simplest methods are those that involve the use of the science camera, in conjunction with algorithms such as Peak-a-boo[11] or Borde and Traub's method[13]. One disadvantage of these, however, is that speckles in the image plane are blurred in broadband light, and hence the performance suffers with bandwidth. An alternative that is not sensitive to bandwidth is to image the pupil plane after the star occulter. The price is additional complexity and possible slight loss of throughput. However, both of these methods work with light after the star occulter and, therefore, do not get a lot of photons. Guyon proposed that light blocked by the star occulter can be used to estimate low-order aberrations. A variation on this theme is to use the light reflected off the shaped pupil. Both of these schemes can be used in addition to the first two mentioned.

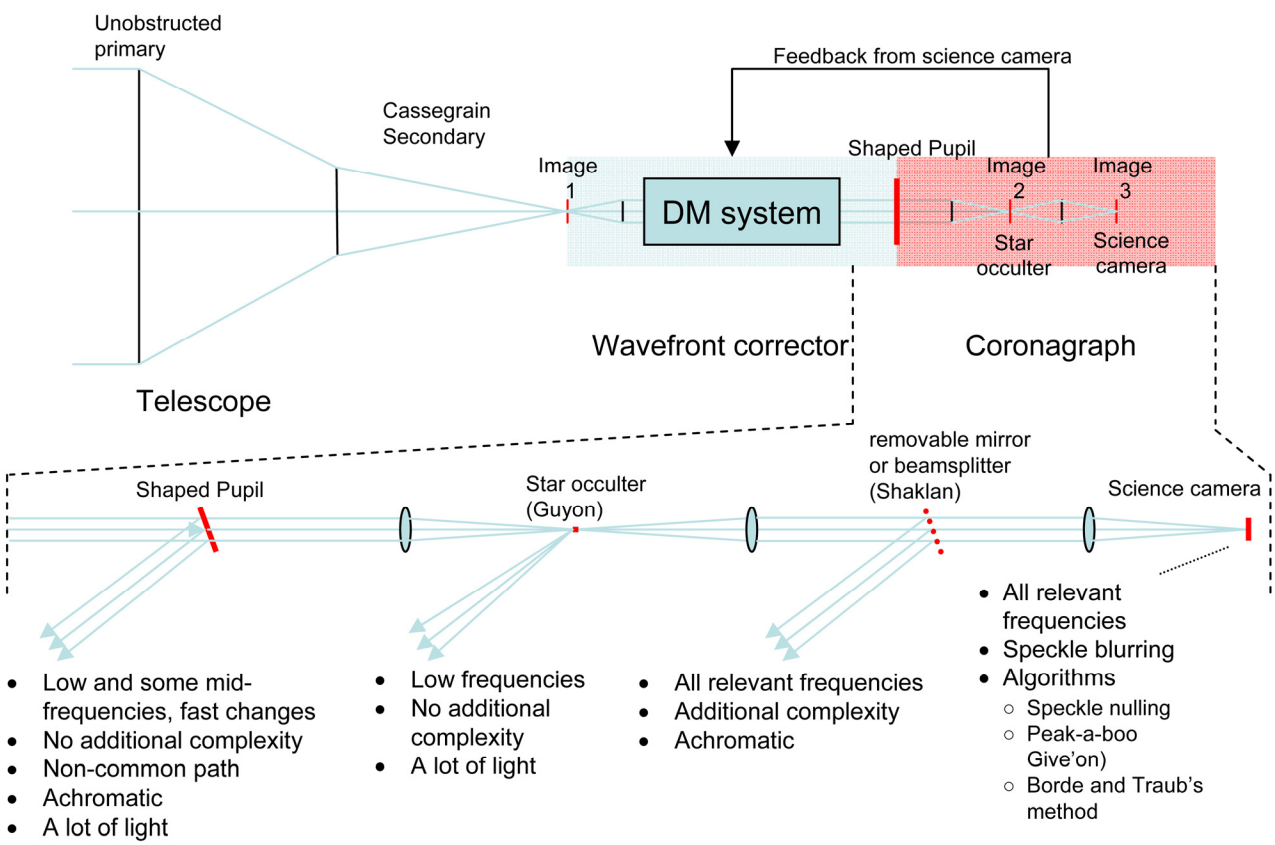

Figure 6: *Schematic diagram of wavefront sensing options.*

The ability to sense and correct for aberrations all the way to 10^{10} contrast in a SPC system that has real masks like those already manufactured today has already been shown theoretically in monochromatic light. Figure 7 shows a simulation of Peak-a-boo estimation and subsequent correction (assuming an ideal DM), in a system having phase and amplitude errors as well as the observed manufacturing errors (trimming) on the mask.

Such corrections work well for monochromatic light, or even in polychromatic light assuming no wavelength dependence of aberrations. However, in reality, both phase and amplitude error will have a non-negligible dependency on wavelength, due to a variety of mechanisms[15], severely limiting the bandwidth across which aberrations can be fully corrected. Nonetheless, in such cases, the required 10^{10} contrast can still be achieved with the SPC if one uses more than 1 DM for correction. Figure 8 shows some possible configurations of 2 and 3 DMs designed to correct for wavelength-dependent errors along with a simulation of correcting for such errors with a 3-DM correction system.

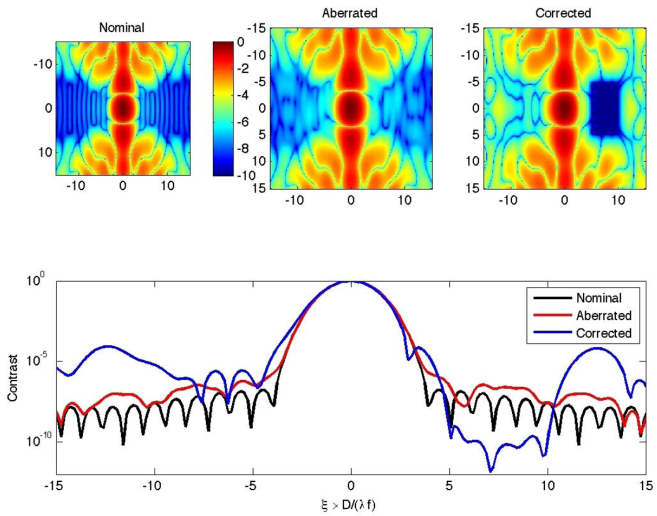

Figure 7: *Demonstration of Peak-a-boo sensing and correction with a realistic shaped pupil having manufacturing defects (trimming), in monochromatic light.*

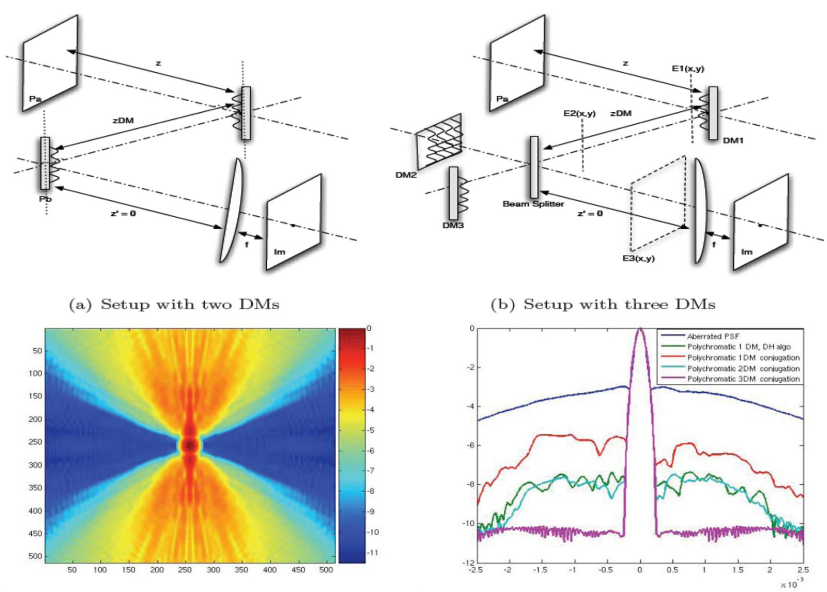

(a) Polychromatic correction with three DM $\Delta\lambda = 400$ nm (b) Slices of the several polychromatic PSFs presented above $\Delta\lambda = 400$ nm

Figure 8: *Top: Multi-DM configurations that allow corrections for realistic wavelength-dependent errors. Bottom: Even a severe case where wavelength-dependent aberrations limit the contrast to 10^3 can be fully corrected by a system of 3 DMs. In this simulation, perfect estimation of the aberrations is assumed.*

ACKNOWLEDGEMENTS

The Princeton group gratefully acknowledges the support of the National Aeronautics and Space Administration through the Jet Propulsion Laboratory, as well as the Michelson Science Center, California Institute of Technology for this work.

REFERENCES

1. Kasdin, N. J., Belikov, R., Beall, J., Vanderbei, R. J., Littman, M. G., Carr, M., & Give'on, A., "Shaped Pupil Coronagraphs for Planet Finding: Optimization, Manufacturing, and Experimental Results," *Proc. of SPIE* 5905, G1-G8, (2005).
2. Kasdin, N. J., Vanderbei, R. J., Spergel, D. N., & Littman, M. G., "Extrasolar Planet Finding via Optimal Apodized and Shaped Pupil Coronagraphs," *Astrophysical Journal* 582, 1147-1161, (2003).
3. Vanderbei, R. J., Kasdin, N. J., & Spergel, D. N., "Checkerboard-Mask Coronagraphs for High-Contrast Imaging," *Astrophysical Journal* 615(2004).
4. Balasubramanian, K., et al., "Fabrication and Characteristics of Free Standing Shaped Pupil Masks for TPF-Coronagraph," *Proc. of SPIE*, 6265 (2006).
5. Ceperley, Daniel; Neureuther, Andrew; Miller, Marshall; Lieber, Michael; Kasdin, Jeremy, "Stray-light sources from pupil mask edges and mitigation techniques for the TPF Coronagraph," *Proc. of SPIE*, 6271(2006).
6. Lieber, Mike; Neureuther, Andrew R.; Ceperley, Dan; Kasdin, Jeremy; Hoppe, Dan; Eisenman, Allan, " Evaluating the end-to-end performance of TPF-C with vector propagation models: Part I. Pupil mask effects," *Proc. of SPIE*, 5906 (2005).
7. Belikov, R., Kasdin, N. J., Vanderbei, R. J., "Diffraction-based Sensitivity Analysis of Apodized Pupil-mapping Systems," *Astrophysical Journal* 652 (2006).
8. Shaklan, Stuart B.; Green, Joseph J., "Low-Order Aberration Sensitivity of Eighth-Order Coronagraph Masks," *Astrophyciscal Journal* 628 (2005).
9. Belikov, Ruslan; Give'on, Amir; Trauger, John T.; Carr, Michael; Kasdin, N. J.; Vanderbei, Robert J.; Shi, Fang; Balasubramanian, Kunjithapatham; Kuhnert, Andreas, "Toward 10^{10} contrast for terrestrial exoplanet detection: demonstration of wavefront correction in a shaped-pupil coronagraph," *Proc. of SPIE*, 6265 (2006).
10. Belikov, Ruslan; Beall, James; Carr, Michael; Give'On, Amir; Kay, Jason; Kolade, Taofik; Littman, Michael; Mycroft, Frank; Pueyo, Laurent; Vanderbei, Robert J.; Kasdin, N. Jeremy, " Towards 10^{10} Contrast for NASA's Terrestrial Planet Finder Mission: Demonstration of High Contrast in a Shaped-Pupil Coronagraph at Princeton," Proceedings of the IAU Colloquium #200, pp. 415-420, 2006.
11. Give'On, Amir; Kasdin, N. Jeremy; Vanderbei, Robert J., "Closed-loop Wavefront Correction for High Contrast Imaging: The ``peak-a-boo" Algorithm," *Proceedings of the IAU Colloquium #200*, pp. 541-546, 2006.
12. Trauger, J., et al., "Coronagraph Contrast Demonstrations with the High Contrast Imaging Testbed," *Proc. of SPIE* 5487, 1330-1336, (2004).
13. Bordé, Pascal J.; Traub, Wesley A., "High-Contrast Imaging from Space: Speckle Nulling in a Low-Aberration Regime," *Astrophysical Journal,* 638 (2006).
14. Guyon, O.; Pluzhnik, E. A.; Kuchner, M. J.; Collins, B.; Ridgway, S. T., "Theoretical Limits on Extrasolar Terrestrial Planet Detection with Coronagraphs," *Astrophysical Journal Supplement Series,* 167, (2006).
15. Shaklan, Stuart B.; Green, Joseph J.; Palacios, David M., "The terrestrial planet finder coronagraph optical surface requirements," *Proc. of SPIE,* 6265 (2006).